Fish & Shellfish Immunology 33 (2012) 753–765

Contents lists available at SciVerse ScienceDirect

Fish & Shellfish Immunology

journal homepage: www.elsevier.com/locate/fsi

A manganese superoxide dismutase (MnSOD) from *Ruditapes philippinarum*: Comparative structural- and expressional-analysis with copper/zinc superoxide dismutase (Cu/ZnSOD) and biochemical analysis of its antioxidant activities

Navaneethaiyer Umasuthan [a], S.D.N.K. Bathige [a], Kasthuri Saranya Revathy [a], Youngdeuk Lee [a], Ilson Whang [a], Cheol Young Choi [b], Hae-Chul Park [c,**], Jehee Lee [a,d,*]

[a] Department of Marine Life Sciences, School of Marine Biomedical Sciences, Jeju National University, Jeju Special Self-Governing Province 690-756, Republic of Korea
[b] Division of Marine Environment and Bioscience, Korea Maritime University, Busan 606-791, Republic of Korea
[c] Graduate School of Medicine, Korea University, Ansan, Gyeonggido 425-707, Republic of Korea
[d] Marine and Environmental Institute, Jeju National University, Jeju Special Self-Governing Province, 690-814, Republic of Korea

ARTICLE INFO

Article history:
Received 10 March 2012
Received in revised form
13 June 2012
Accepted 28 June 2012
Available online 10 July 2012

Keywords:
Ruditapes philippinarum
Manganese superoxide dismutase (MnSOD)
Copper/znic superoxide dimutase (Cu/ZnSOD)
Gene expression
Antioxidant activity

ABSTRACT

Superoxide dismutases (SODs), antioxidant metalloenzymes, represent the first line of defense in biological systems against oxidative stress caused by excessive reactive oxygen species (ROS), in particular $O_2^{\bullet-}$. Two distinct members of SOD family were identified from Manila clam *Ruditapes philippinarum* (abbreviated as RpMnSOD and RpCu/ZnSOD). The structural analysis revealed all common characteristics of SOD family in both RpSODs from primary to tertiary levels, including three MnSOD signatures and two Cu/ZnSOD signatures as well as invariant Mn^{2+}- and Cu/Zn^{2+}-binding sites in RpMnSOD and RpCu/ZnSOD, respectively. Putative RpMnSOD and RpCu/ZnSOD proteins were predicted to be localized in mitochondrial matrix and cytosol, respectively. They shared 65.2% and 63.9% of identity with human MnSOD and Cu/ZnSOD, respectively. Phylogentic evidences indicated the emergence of RpSODs within molluscan monophyletic clade. The analogous spatial expression profiles of *RpSOD*s demonstrated their higher mRNA levels in hemocytes and gills. The experimental challenges with poly I:C, lipopolysaccharide and *Vibrio tapetis* illustrated the time-dependent dynamic expression of *RpSOD*s in hemocytes and gills. The recombinant RpMnSOD was expressed in a prokaryotic system and its antioxidant property was studied. The rRpMnSOD exhibited its optimum activity at 20 °C, under alkaline condition (pH 9) with a specific activity of 3299 U mg^{-1}. These outcomes suggested that RpSODs were constitutively expressing inducible proteins that might play crucial role(s) in innate immunity of Manila clam.

1. Introduction

The Manila clam *Ruditapes philippinarum* is one of the valuable aquacrop in commercial fisheries. However, mass mortalities caused by *Vibrio tapetis* infection resulting in brown ring disease have been widely recognized as one of the major reason for enormous economic losses to the clam aquaculture [1]. Hence, understanding the defense strategies of immune system in clam may facilitate the development of a highly sustainable clam industry. The lack of adaptive immunity makes clams exclusively depend on innate immunity, to shield themselves from microorganisms abundant in marine environment. When the external defense layers are breached by pathogens, the humoral- and cellular-defenses are activated to eradicate the invading pathogens. The hemocyte-mediated phagocytosis is considered to be the main strategy in cellular-defenses of invertebrates [2]. During this defense response, increased O_2 consumption in turn generates reactive oxygen species (ROS), such as $O_2^{\bullet-}$, H_2O_2 and $^{\bullet}OH^{-}$. Although these ROS play critical roles in signaling pathways [3], they could damage macromolecules and cause cellular dysfunctions at elevated levels. Hence, rapid removal of excessive ROS is necessary to withstand the cellular homeostasis. Many antioxidant defense schemes have evolved in biological systems to maintain the redox balance.

Among the antioxidant enzymes, the superoxide dismutases (SODs; EC 1.15.1.1) are considered to be the first line of defense against oxidative stress, since they convert $O_2^{\bullet-}$ to O_2 and H_2O_2 [4],

* Corresponding author. Marine Molecular Genetics Lab, Department of Marine Life Sciences, College of Ocean Science, Jeju National University, 66 Jejudaehakno, Ara-Dong, Jeju 690-756, Republic of Korea. Tel.: +82 64 754 3472; fax: +82 64 756 3493.
** Corresponding author. Tel.: +82 31 412 6712; fax: +82 31 412 6729.
E-mail addresses: hcpark67@korea.ac.kr (H.-C. Park), jehee@jejunu.ac.kr (J. Lee).

1050-4648/$ – see front matter © 2012 Elsevier Ltd. All rights reserved.
http://dx.doi.org/10.1016/j.fsi.2012.06.024

which is subsequently transformed into H_2O by catalase. The SOD family is ubiquitously distributed in almost all forms of aerobic lives and classified into four classes based on associated metal cofactors, namely copper/zinc SOD (Cu/ZnSOD), manganese SOD (MnSOD), iron SOD (FeSOD) and nickel SOD (NiSOD). Regardless of their stable basal expression in normal physiology, SOD transcription is known to be governed by a diverse number of internal and external stress-stimuli [5].

The compartmentalization of each SOD type in the cell varies. In principal, Cu/ZnSOD and MnSOD are localized to cytoplasm and mitochondrial matrix, respectively. While Cu/ZnSOD acts as a bulk scavenger of $O_2^{\bullet-}$ in the intracellular environment, MnSOD plays its antioxidant role in mitochondria. The significance of SODs in immune defense is emerging based on evidences indicating the modulation of SOD expression by endotoxins [6,7] and pathogens [8–10]. Despite a number of previous endeavors reporting the identification of *MnSOD*s [11,12] and *Cu/ZnSOD*s [7,13] from aqua invertebrates, their expression has been rarely profiled against immune challenges in a comparative perspective [10].

In the present study, we identified two *SOD*s denoted as *RpMnSOD* and *RpCu/ZnSOD*, of which the latter was similar to a previously reported partially characterized homolog [14]. The current study was designed with the following aims: (1) to characterize the identified SODs at molecular structural levels, (2) to elucidate their comparative gene expression at transcript level in healthy animals to determine basal-tissue expression, as well as in clams administered with poly I:C, LPS and *V. tapetis* to demonstrate any changes in the *in vivo* basal-expression and (3) to clone *RpMnSOD* and express the protein *in vitro* to characterize the recombinant protein at functional level using antioxidant assays.

2. Materials and methods

2.1. Isolation of RpSOD cDNAs from Manila clam cDNA library

A cDNA library of Manila clam was constructed using RNA isolated from multiple tissues of healthy animals. The procedure of cDNA library construction, normalization and initial GS-FLX™ sequencing strategies have been described in our previous report [15]. The cDNA sequences were randomly selected and subjected to DNA sequence analysis. Two cDNA clones were found to have the full lengths of *MnSOD* and *Cu/ZnSOD* with 5′- and 3′-untranslated regions (UTRs) and designated as *R. philippinarum MnSOD* (*RpMnSOD*) and *Cu/ZnSOD* (*RpCu/ZnSOD*), respectively.

2.2. Bioinformatic analysis of RpSOD sequences

The cDNA and amino acid sequences of RpSODs were analyzed using the BLAST program at the NCBI (http://blast.ncbi.nlm.nih.gov/Blast) and the ExPASy resource portal (http://expasy.org/), respectively. Proteomic parameters of RpSODs were retrieved using ProtParam tool. Characteristic domains or signature motifs were identified using the SMART (http://smart.embl-heidelberg.de/) or PROSITE database (http://prosite.expasy.org/scanprosite/). Probability to be exported to mitochondria was determined by using the Predotar Server (http://urgi.versailles.inra.fr/predotar/predotar.html). N-Glycosylation sites were deduced using NetNGlyc 1.0 server (http://www.cbs.dtu.dk/services/NetNGlyc/). The homologous SOD members were retrieved from GenBank and used in calculating the identity and similarity percentages with RpSODs by applying EMBOSS pairwise alignment algorithms (http://www.ebi.ac.uk/Tools/emboss/align/). Amino acid sequence alignment of Manila clam and other known SODs was performed using the ClustalW program. The 3D structures of RpSODs were predicted by using SWISS-MODEL and I-TASSER protein modeling servers [16,17], and human -MnSOD and -Cu/ZnSOD (PDB IDs: 1luvB and 1n19B) were selected as structural templates. The constructed theoretical models were visualized using Rasmol (2.7.5.2) and DeepView (4.0.1). The phylogenetic tree was constructed based on amino acid sequences by applying the Neighbor-Joining (NJ) algorithm using MEGA 5 program.

2.3. Animals

Manila clams with an average size of 35 ± 5 mm were collected from the Seongsan beach located in Jeju Island (Republic of Korea) and reared in 80 L tanks of continuously aerated sand-filtered seawater (34 ± 1‰, 21 ± 1 °C). After one week of acclimation, clams were used for the challenge experiments.

2.4. Injection of stimulants and bacterial pathogen

In order to investigate the response of *RpSOD*s against stimulants and bacterial infection, three challenges were devised in time course experiments using LPS (*Escherichia coli* 0127:B8; Sigma–Aldrich), poly I:C (Sigma–Aldrich) and a Gram-negative bacterium *V. tapetis*, as described previously [15]. Briefly, two clam groups were injected with either LPS and poly I:C (100 μg clam^{-1}) suspended in saline (0.9% NaCl). The *V. tapetis* [KCTC no. 12728] was obtained from the Korean Collection for Type Culture (KCTC). The bacterium was cultured, resuspended in saline and intramuscularly injected (1.9×10^8 cells clam^{-1}) into adductor muscle of clams belong to the third group. An un-injected group was established as negative control, while a group injected with an equal volume (100 μL) of saline served as positive control.

2.5. Tissue and hemolymph sampling, total RNA isolation and cDNA construction

In order to evaluate the expression of the *RpMnSOD* and *RpCu/ZnSOD* mRNA under normal physiological conditions, adductor muscle, mantle, siphon, gill and foot tissues were isolated from five healthy individuals. Hemolymph (1–2 mL animal^{-1}) was also collected from each clam using an aseptic syringe and immediately centrifuged at 3000 *g* for 10 min at 4 °C to harvest the hemocytes. To determine the defense responses of *RpSOD*s, hemocytes and gill tissues were removed at 3, 6, 12, 24 and 48 h post-injection (p.i.) from control and each challenged groups and kept at −80 °C until use.

Total RNA was extracted from above tissues collected from normal and challenged clam groups using Tri Reagent™ (Sigma–Aldrich). The single-strand cDNA was synthesized based on manufacturer's instructions of PrimerScript™ 1st Strand cDNA Synthesis Kit (Takara) using total RNA as template. Synthesized cDNA was diluted to 1:40 and stored at −20 °C for subsequent quantitative RT-PCR (qRT-PCR).

2.6. Spatial and temporal expression analysis of two clam SOD genes by qRT-PCR

The expression pattern of *RpSOD*s in different tissues from healthy group and challenged groups was detected by qRT-PCR. The gene-specific primers were designed for *RpMnSOD, RpCu/ZnSOD* and *β-actin* (Table 1). The *β-actin* was used as an internal control to verify the qRT-PCR reaction and adjust the cDNA templates. Assays were performed in triplicates of 20 μL reaction system containing 4 μL of diluted cDNA, 10 μL of 2 × Takara SYBR premix Ex *Taq*™, 0.8 μL of each primer (10 pmol μL^{-1}), and 5 μL dH_2O. The qRT-PCR program consisted of a single denaturation step at 95 °C for 10 s, followed by 45 amplification cycles of 95 °C for 5 s, 58 °C for 10 s, and 72 °C for 20 s; and a final single cycle of 95 °C for 15 s, 60 °C for

Table 1
Description of primers used in this study.

Name	Purpose	Primer sequence (5′→3′)[a]
RpMnSOD-F	CDS amplification (*Eco*RI)	$(GA)_3$gaattcATGCTGTCAGC TCAAAGTGTTAAGCTT
RpMnSOD-R	CDS amplification (*Hind*III)	$(GA)_3$gtcgacCTAGGCAT CCAGTCGGGCTT
RpMnSOD-F	RT-PCR amplification	AAGGACATGTTGACAC AGGCTTCG
RpMnSOD-R	RT-PCR amplification	AAAGCCTGTTGTTGGTT GCAGAGG
RpCu/ZnSOD-F	RT-PCR amplification	GTGCAGGTCCTCACTAT AACCCA
RpCu/ZnSOD-R	RT-PCR amplification	GACAACTCGTGACCACC TTTACC
Rp-β-actin-F	RT-PCR internal reference	CTCCCTTGAGAAGAGCT ACGA
Rp-β-actin-R	RT-PCR internal reference	GATACCAGCAGATTCCAT ACCC

F, forward; R, reverse.
[a] Lowercase letters indicate restriction enzyme target sequence introduced. Number of the same base pair repeats was given within bracket with subscripted number.

30 s, and 95 °C for 15 s. To determine *RpSOD* mRNA expression levels, the comparative CT method ($2^{-\Delta\Delta CT}$ method) was used. In spatial distribution analysis, the expression level of *RpSOD*s in adductor muscle was used as the basal value, to which the expression levels in all other tissues were compared. In temporal expression analysis, fold-change p.i. was determined by comparing with the expression in unchallenged- as well as corresponding time-matched saline-control groups.

2.7. Construction of the expression plasmid

The coding sequence (CDS) of *RpMnSOD* was amplified using Ex Taq DNA polymerase (Takara) and specific primers for the 5′- and 3′-end of the *RpMnSOD* cDNA appended with restriction sites for *Eco*RI and *Hind*III, respectively (Table 1). The PCR product was purified using the Accuprep® PCR purification kit (Bioneer Co.), and digested with the endonucleases. The précised fragment was excised from electrophoretically resolved digested products and refined using the Accuprep® gel purification kit (Bioneer Co.). Subsequently, it was ligated into pMAL-c2X expression vector (New England Biolabs), and the recombinant plasmid pMAL-c2X/RpMnSOD was transformed into *E. coli* DH5α cells. Sequence confirmed construct was retransformed into *E. coli* BL21 (DE3) cells.

2.8. Prokaryotic expression and purification of recombinant RpMnSOD (rRpMnSOD)

A starter culture was inoculated into rich medium containing 100 μg mL^{-1} of ampicillin and 0.2% of glucose, and incubated at 37 °C with shaking at 150 rpm. When the OD_{600} of bacterial culture reached ~0.6, isopropyl-β-thiogalactopyranoside (IPTG) was added into medium at a final concentration of 0.25 mM, and then continued to incubate for 20 h at 17 °C to induce the recombinant protein expression. The cells were cultivated by centrifugation (3500 rpm for 30 min at 4 °C) and resuspended in column buffer (20 mM Tris–HCl, 200 mM NaCl; pH 7.4) before stored at −20 °C for overnight. Following day, cells were thawed on an ice-water bath and subjected to cold sonication after incubation with lysozyme for 1 h on ice. The lysate was centrifuged (9000 *g* for 30 min at 4 °C) to obtain the crude extract of the recombinant protein which was then subjected to an affinity column chromatography technique, as described in the pMAL protein fusion and purification protocol (NEW ENGLAND BioLabs® Inc.) [18]. All the subsequent purification steps were conducted at 4 °C. The crude enzyme extract was mixed with pre-washed amylose resin and placed on ice to facilitate the affinity binding. Then, extract-resin mixture was loaded onto a 1 × 5 cm column and washed with 12 × volume of column buffer. Finally, by applying 5 mL of elution buffer (column buffer + 10 mM maltose) to the column, rRpMnSOD was eluted in 0.5 mL aliquots. The concentration of the purified rRpMnSOD was determined with respect to bovine serum albumin standard by Bradford method. The purity and molecular mass of the protein preparation were evaluated by subjecting the purified protein on 12% SDS–PAGE and stained with 0.05% Coomassie brilliant blue R-250.

2.9. Identification of rRpMnSOD using mass spectrometry

In order to verify the amino acid sequence of the rRpMnSOD, the rRpMnSOD-MBP fusion protein separated on SDS-PAGE was subjected to mass spectrometry. After CB-R250 staining, the gel bearing the fusion protein was excised into 1 mm blocks. By washing the gel blocks with equal volume mixture of 10 mM NH_4HCO_3 and 50% CH_3CN, CB-R250 was removed. By applying 100% CH_3CN, they were dehydrated and vacuum dried. Subsequently, gel blocks were digested using 125 ng of sequencing-grade trypsin (Promega) as per manufacturer's recommendations. The aqueous phase of the digestion reaction was separated and lyophilized. Then, lyophilized tryptic peptides were suspended in 0.1% formic acid and analyzed by Nano-LC/ESI-MS/MS (Korea Basic Science Institute). The obtained data were further analyzed against deduced sequence of rRpMnSOD-MBP fusion protein using the Mascot tool.

2.10. Antioxidant activity of rRpMnSOD

A modified procedure from a previous report was adopted in determining the antioxidant activity of purified recombinant RpMnSOD [19]. In the assay system, $O_2^{\bullet-}$ generated by xanthine oxidase (XOD) during the conversion of xanthine to H_2O_2 and uric acid in turn transforms nitroblue tetrazolium (NBT) to NBT-diformazan dye that enables the system to absorb light at 560 nm. SOD competes for $O_2^{\bullet-}$ and reduces the level of $O_2^{\bullet-}$ in system. The subsequent reduction in formation of NBT-diformazan is used as a measure of SOD activity. Briefly, assay was performed in triplicates on a 96 well plate. Each well contained 160 μL of 0.1 M glycine-NaOH buffer (pH 9), 6.75 μL of each xanthine (3 mM), EDTA (3 mM), BSA (0.15%), NBT (0.75 mM), and 20 μL rRpMnSOD. After equilibration at 20 °C for 10 min, the reaction was initiated by adding 6 mU of XOD and incubated further at 20 °C for 20 min. The reaction was terminated by addition of 6.75 μL of 6 mM CuCl and absorbance at 560 nm was determined using a microplate reader (Multiskan EX, Thermo Scientific). The effect of MBP fusion protein on rRpMnSOD activity also was measured as a control. One unit enzyme activity was defined as the amount of enzyme required to decrease the formation of diformazan dye by 50% and specific activity as unit (U) mg^{-1} protein.

2.11. Biochemical properties of rRpMnSOD

To characterize the biochemical properties of rRpMnSOD, XOD assay was performed under different temperature and pH conditions. Reaction was assayed from 15 to 60 °C and pH from 3 to 11 in different intervals to determine the optimal -temperature and -pH, respectively. Different buffers namely citrate (pH 3, 4, 5), phosphate (pH 6, 7, 8), and glycine–NaOH (pH 9, 10, 11) were used in determination of optimal pH. The relative enzyme activity was calculated as a percentage (%) by considering the mean values of triplicate reactions. Relative activity = (respective activity/highest activity) × 100%.

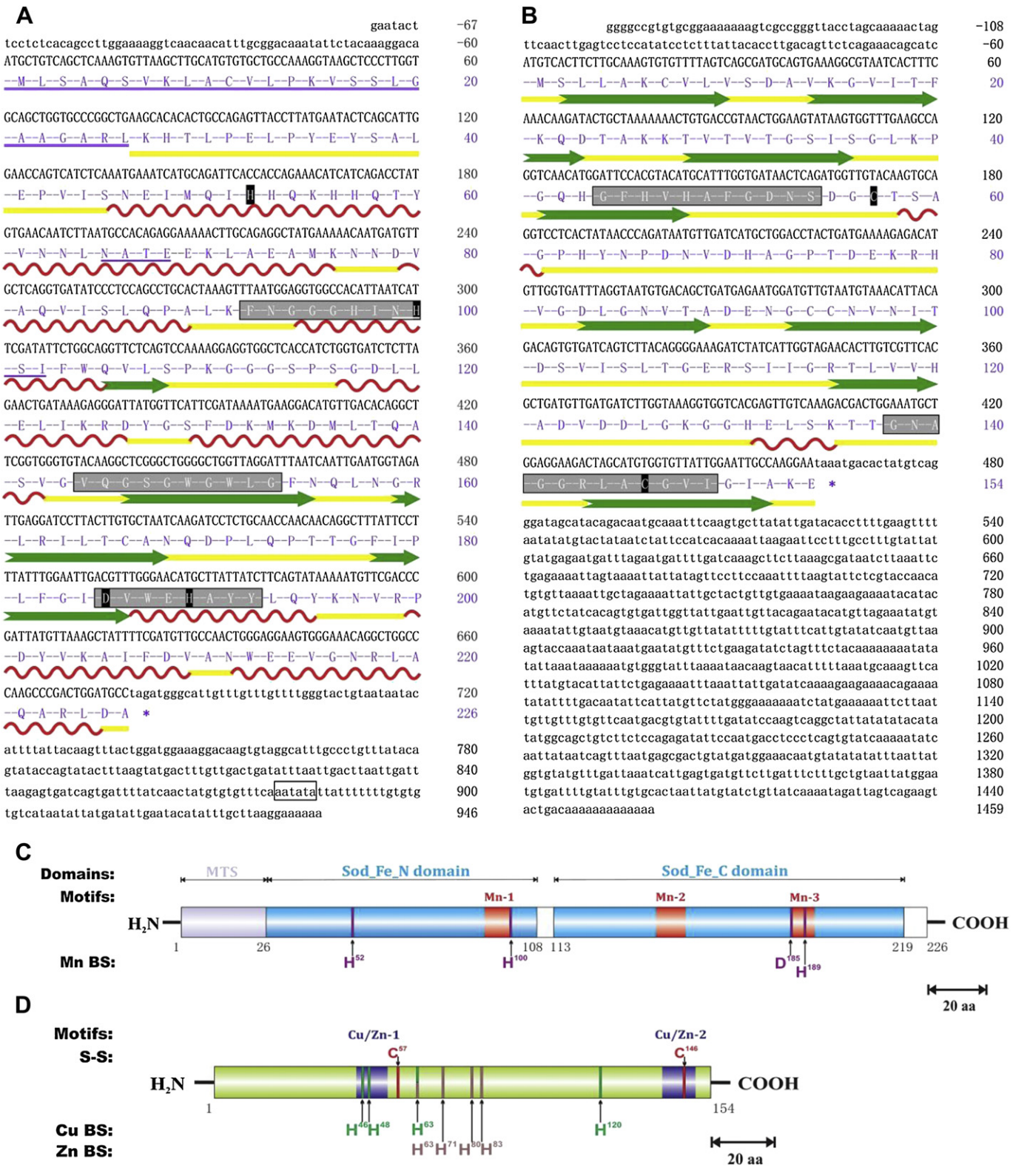

Fig. 1. Nucleotide and the deduced amino acid sequences of *R. philippinarum* (A) MnSOD and (B) CuZnSOD. Stop codons are marked with asterisks. Polyadenylation signal is enclosed in a rectangle and mRNA instability motifs are shown in bold face. Potential *N*-glycosylation sites of RpMnSOD are underlined. Predicted MTS is double underlined. Putative family signature motifs are shaded in gray. Potential Mn^{2+}-binding sites (Mn-BS) in RpMnSOD and two C residues forming a disulfide bridge in RpCu/ZnSOD are shaded in black. Secondary structural features are presented below each amino acid sequence: yellow line, coil; red wave, α-helix; green arrow, β-strand. (C) The domain architecture of RpMnSOD is composed of a MTS (gray), a Sod_Fe_N_domain and Sod_Fe_C_domain (blue). Signature motifs (red) and Mn-BS (purple) are also marked. (D) The domain architecture of RpCu/ZnSOD is composed of two signature motifs (purple), four Cu-BS (green) and four Zn-BS (brown). S-S, disulfide bond; BS, binding site. (For interpretation of the references to colour in this figure legend, the reader is referred to the web version of this article.)

2.12. Statistical analysis

All the results were reported as mean ± standard deviation (SD) of triplicates. Intergroup differences were analyzed by unpaired, two-tailed *t*-test to compare the means using GraphPad program (GraphPad Software, Inc.). Differences were considered to be significant at $P < 0.05$ and extremely significant at $P < 0.01$.

3. Results

3.1. Molecular characterization of two RpSODs

3.1.1. cDNA- and protein- sequences of RpSODs

Two putative cDNAs representing superoxide dismutases were identified from the Manila clam cDNA library (contigs 36025 and 83766) based on their similarity to previously reported SOD members and designated *RpMnSOD* and *RpCu/ZnSOD*. The Cu/ZnSOD identified in this study varied from a previously reported isoform (GQ384412) by 3 bp and an amino acid [14], and the characterization data of *RpCu/ZnSOD* are provided in appendix. The nucleotide and amino acid sequences of RpMnSOD and RpCu/ZnSOD shown in Fig. 1 have been deposited in GenBank (Accession numbers, JN593115 and JQ362416), respectively. The full-length *RpMnSOD* cDNA comprised of 1013 bp, containing a 5′-untranslated region (UTR) of 67 bp, a CDS (including stop codon, TAG) of 681 bp and a 3′-UTR of 265 bp with two mRNA instability motifs (^{887}ATTTA^{891} and ^{905}ATTTA^{909}) and a putative polyadenylation signal sequence (^{947}AATATA^{952}) (Fig. 1A). The CDS of *RpMnSOD* was translated to a product of 226 amino acids with a predicted molecular weight of 25069 and a theoretical *p*I of 6.7. Prediction analysis of the identified protein revealed the presence of a 26 amino acid long mitochondrial targeting sequence (MTS) at N-terminal suggesting its localization to the mitochondria. There were two potential sites for *N*-glycosylation (^{65}NATE^{68} and ^{99}NHSI^{102}) in the RpMnSOD. SMART program revealed the presence of two conserved domains of Sod_Fe_N (27–108) and Sod_Fe_C (113–219). A comparative analysis revealed three potential MnSOD-family signature motifs (^{92}FNGGGHINH^{100}, ^{144}VQGSGWGWLG^{153} and ^{185}DVWEHAYY^{192}) and four putative Mn^{2+}-binding sites (H^{52}, H^{100}, D^{185} and H^{189}) which mediate its catalytic activity (Fig. 1C). Supplementary Table 1 shows the characteristic features of RpCu/ZnSOD (Fig. 1B, D).

3.1.2. Comparative analysis of two RpSOD protein sequences

Furthermore, amino acid sequences of RpSODs were compared with SODs of other known species. It was revealed that RpMnSOD and RpCu/ZnSOD revealed an overall identity ranging from ~60% to 70% and ~58%–66%, where the highest identities were demonstrated with *Mizuhopecten yessoensis* MnSOD (69.9%) and *Mactra veneriformis* Cu/ZnSOD (66.5%), respectively (Table 2). Alignment studies conducted using eight different SOD members including RpSODs demonstrated the completely (100%) conserved regions in RpMnSOD (Fig. 2A) and RpCu/ZnSOD (Fig. 2B), including the Mn and Cu/Zn family signature motifs, invariant amino acids responsible for the coordination of Mn and Cu/Zn, and two cysteines (C^{57} and C^{146}) that form a disulfide bond respectively.

3.1.3. 3D structural modeling of two RpSODs

Based on human MnSOD and Cu/ZnSOD protein templates, which shared 72.3% and 67.1% of identity with corresponding clam SODs, the potential tertiary structures of RpSODs were constructed (Fig. 3). The homology models of RpSODs (Fig. 3A and C) revealed their distinctiveness in structural identity, 3D folding and evolutionary conservation of the active sites such as Mn^{2+} (H^{52}, H^{100}, D^{185} and H^{189}) in RpMnSOD (Fig. 3B), Cu^{2+} (H^{46}, H^{48}, H^{63}, and H^{120}) (Fig. 3D) and Zn^{2+} (H^{63}, H^{71}, H^{80} and D^{83}) (Fig. 3E) in RpCu/ZnSOD with respect to the human SODs.

3.1.4. Molecular phylogeny of two RpSOD proteins

To evaluate the molecular evolutionary relationship of RpSODs, the sequences of known SOD members from representative species were selected to construct the phylogenetic trees by NJ method. The tree of MnSOD members diverged into two major groups namely mitochondrial- and cytosolic-MnSODs. RpMnSOD was positioned within molluscan cluster of mitochondrial branch, maintaining a distinct position from the sister group of other bivalves (Fig. 4A). However, phylogeny analysis of Cu/ZnSOD members placed the RpCu/ZnSOD within molluscan cluster close to that of surf clam (Fig. 4B). This indicates that both RpSODs are derivatives of respective common ancestors similar to other invertebrate homologs [5].

3.2. Expressional characterization of two RpSODs at mRNA level

3.2.1. Spatial expression and differential distribution of RpSODs

To investigate the tissue distribution profile of two *RpSOD* transcripts, total RNA from the tissues of gills, hemocytes, mantle, foot, siphon and adductor muscle was extracted from healthy clams. The qRT-PCR analysis was performed using Manila clam *β-actin* as an invariant control and relative mRNA expression-fold was derived by comparing the transcript level in each tissue with that of adductor muscle. The results indicated that both *SOD* transcripts

Table 2
Comparative homology analysis of *R. philippinarum* SODs, RpMnSOD and RpCu/ZnSOD with other SODs.

Species	Taxonomy	Mn superoxide dismutase				Cu/Zn superoxide dismutase			
		Accession No	I%	S%	aa	Accession No	I%	S%	aa
R. philippinarum	Bivalvia	JN593115[a]	100.0	100.0	226	ACU83236	99.4	100.0	154
M. yessoensis	Bivalvia	BAE78580	69.9	81.9	226	n.a.	–	–	–
M. veneriformis	Bivalvia	n.a.	–	–	–	ACU46013	66.5	73.9	159
A. irradians	Bivalvia	ABW98672	68.1	79.2	226	ACE76954	63.2	78.1	152
H. discus discus	Gastropoda	ABF67504	65.0	79.6	226	ABG88844	64.5	74.8	154
C. gigas	Bivalvia	ABZ90958	60.5	75.4	225	CAD42722	63.7	75.2	156
C. hongkongensis	Bivalvia	ADR70997	62.3	76.8	225	ADR70998	63.7	75.2	156
B. mori	Insecta	NP_001037299	62.1	74.0	216	BAD69805	62.6	72.9	154
H. mylodon	Teleostei	ACR23311	65.5	73.5	224	ACR56338	58.7	74.2	154
D. rerio	Teleostei	AAP34300	65.0	73.0	224	NP_571369	60.6	74.2	154
X. laevis	Amphibia	AAQ63483	62.2	73.9	230	NP_001080933	58.7	68.4	151
G. gallus	Aves	NP_989542	64.3	72.2	224	AAB88059	62.8	70.5	154
H. sapiens	Mammalia	NP_000627	65.2	73.5	222	NP_000445	63.9	74.8	154
M. musculus	Mammalia	AAB60902	65	75.7	222	NP_035564	62.6	76.1	154

Pair-wise identity percentage was calculated using EMBOSS Needle algorithm with default parameters.
[a] Present study; I, identity; S, similarity; aa, amino acids; n.a., not available.

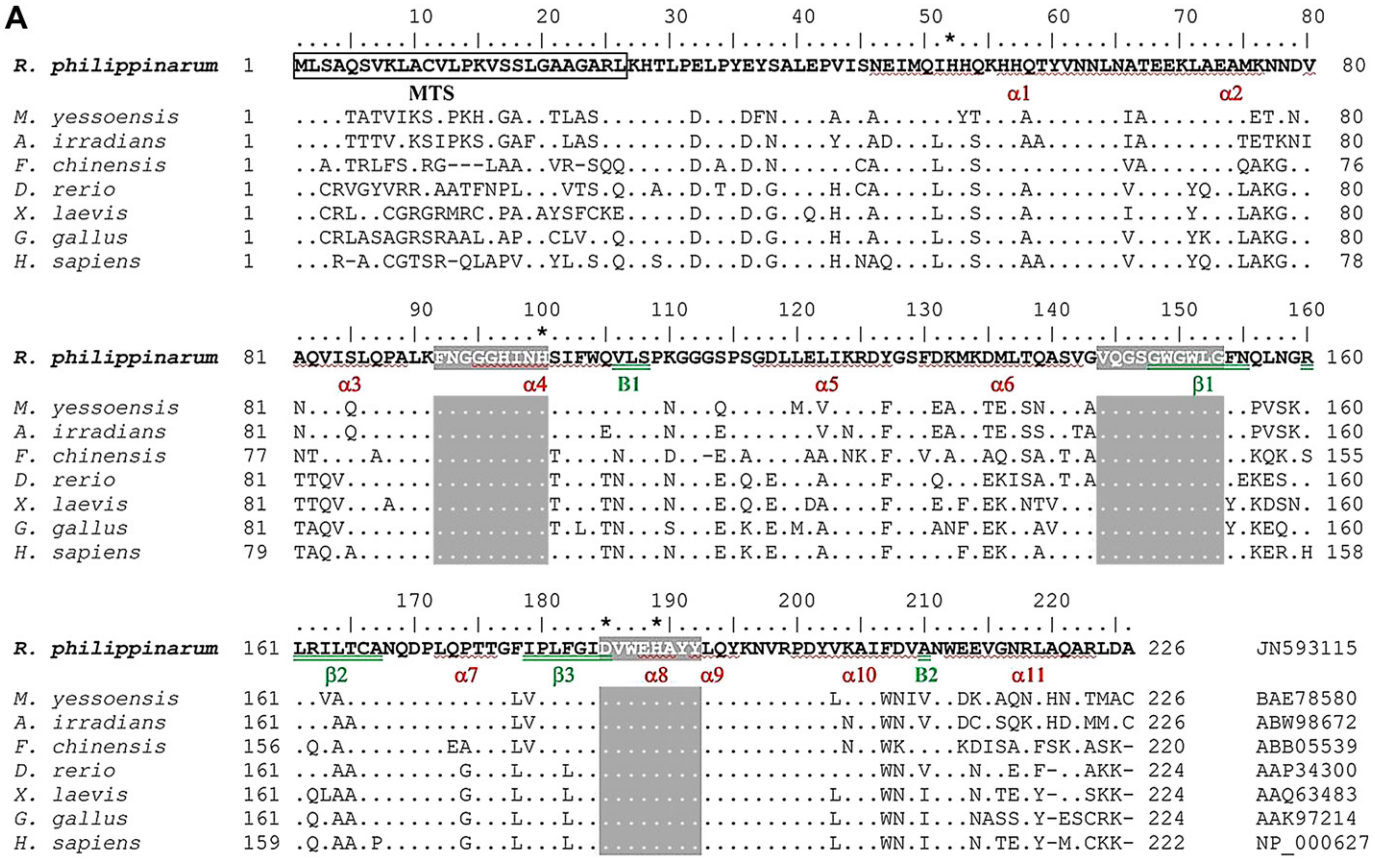
A
R. philippinarum
M. yessoensis
A. irradians
F. chinensis
D. rerio
X. laevis
G. gallus
H. sapiens
MTS
α1
α2
α3
α4
B1
α5
α6
β1
β2
α7
β3
α8
α9
α10
B2
α11
JN593115
BAE78580
ABW98672
ABB05539
AAP34300
AAQ63483
AAK97214
NP_000627

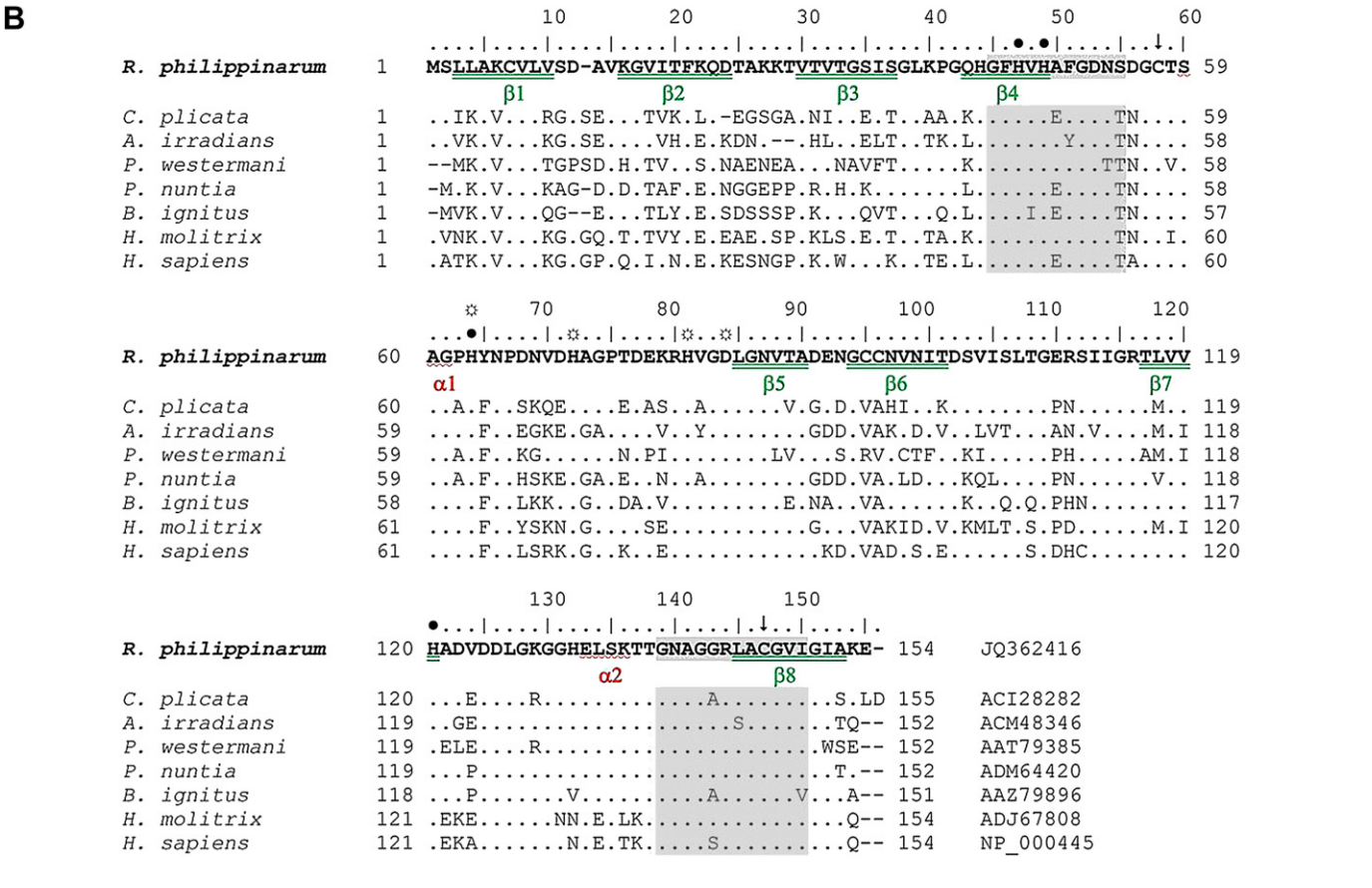
B
R. philippinarum
C. plicata
A. irradians
P. westermani
P. nuntia
B. ignitus
H. molitrix
H. sapiens
β1
β2
β3
β4
α1
β5
β6
β7
α2
β8
JQ362416
ACI28282
ACM48346
AAT79385
ADM64420
AAZ79896
ADJ67808
NP_000445

were constitutively expressed in all examined tissues, but the relative levels of basal expression were variable (Fig. 5). Predominant expression of *RpMnSOD* was detected in hemocytes; in contrast, *RpCu/ZnSOD* was robustly transcribed in gills. Significant transcription of *RpMnSOD* and *RpCu/ZnSOD* was apparently present in gill and hemocytes, respectively. However, the abundance of *RpSOD* mRNAs in other tissues examined was poor.

3.2.2. Temporal transcriptional modulation of two RpSODs after challenges

The time-dependent expression patterns of *RpSOD* mRNAs in hemocytes and gills following the injection of stimulants and a pathogenic bacterium were investigated using qRT-PCR. Mortality was not recorded during the experimental challenges; however, transcription of *RpSOD*s was considerably altered. Interestingly, the modulated mRNA expression levels revealed a significant coordination between two *RpSOD*s through their similar profile patterns following all the challenges.

Fig. 6A and B show the gene expression profiles of *RpSOD*s in poly I:C injected clams. In gills, the transcription levels of *RpMnSOD* and *RpCu/ZnSOD* gradually increased up to 12 h p.i. ($P < 0.01$; 5.8 and 7 fold, respectively) and then steadily reached their basal levels at 48 h p.i. (Fig. 6A). In contrast, the level of *RpMnSOD* and *RpCu/ZnSOD* transcripts in hemocytes exhibited significantly induced expression level at 6 h p.i. ($P < 0.01$) and then showed the highest expression level at 48 h p.i. with 10.1 and 8.1 folds ($P < 0.01$), respectively (Fig. 6B) as a late-phase response.

The LPS p.i. expression profiles of *RpSOD*s are shown in Fig. 6C and D. The expression patterns of the *RpMnSOD* and *RpCu/ZnSOD* transcripts in gills (Fig. 6C) and hemocytes (Fig. 6D) showed significantly highest expression level at 3 h p.i (5.8 and 8.1 fold) and 6 h p.i. (7.1 and 5.4 fold) respectively, after stimulation with LPS ($P < 0.01$).

As shown in Fig. 6E and F, in gills of *V. tapetis* challenged clams, both *RpMnSOD* and *RpCu/ZnSOD* displayed significantly elevated mRNA levels at 6 h p.i. (2.7 fold) and 3 h p.i. (3.8 fold), respectively ($P < 0.01$) (Fig. 6E). Whereas, the maximum induction of *RpSOD* transcript levels in hemocytes was recorded at 24 h p.i. with 2.3 and 2.2 fold, respectively ($P < 0.05$) (Fig. 6F). Interestingly, both *RpSOD*s demonstrated a distinct down-regulation in gills and hemocytes at 48 h and 12 h, respectively ($P < 0.05$). These evidences collectively suggested that temporal expression of *RpSOD*s was tissue-specifically modulated in a stimulant-dependent manner.

3.3. Physiological characterization of RpMnSOD at protein level

3.3.1. Prokaryotic expression and purification of the soluble rRpMnSOD

We introduced the CDS of *RpMnSOD* into pMAL-c2X expression vector and transformed the recombinant construct to express the rRpMnSOD protein in *E. coli* BL21 (DE3) cells through IPTG-mediated induction. The purified protein was analyzed on SDS-PAGE (Fig. 7A). Purified rRpMnSOD fusion protein appeared as a single band with a molecular size of ~68 kDa, which is close to the size of calculated molecular mass of the fusion protein (RpMnSOD, 25 kDa + MBP, 42.5 kDa).

3.3.2. Verification of rRpMnSOD sequence by mass spectrometry

The amino acid sequences of 11 peptide fragments derived from trypsin digestive-treatments of purified rRpMnSOD fusion protein was determined by Nano-LC/ESI-MS/MS and verified with deduced amino acid sequence of rRpMnSOD-MBP fusion protein. The MS determined ~90% of the amino acid residues (204) deduced from cDNA and three short fragments were missing (Table 3). The nominal mass (Mr) of fusion protein was found to be 68023 Da. A polypeptide corresponding to the MBP tag was also identified at N-terminus (Not shown).

3.3.3. The antioxidant potential of rRpMnSOD to dismutate $O_2^{\bullet -}$ radicals

The rRpMnSOD-catalyzed dismutation of $O_2^{\bullet -}$ radicals was determined employing the standard xanthine/XOD method. The reaction was assayed under optimum standard conditions (at 20 °C, pH 9) with different doses (0.625–40 μg) of purified rRpMnSOD and rMBP as a negative control. The catalytic activity of rRpMnSOD was presented as the percentage inhibition of diformazan formation (Fig. 7B). The %-inhibition significantly increased ($P < 0.05$) up to a dose of 2.5 μg and then, exhibited continuous extreme elevation ($P < 0.01$) in a dose-dependent manner. While rRpMnSOD demonstrated ~50% of inhibition at a dose of 40 μg, the control assay performed with MBP indicated no significant inhibition by the fusion-tag. The analysis of results revealed that the specific activity of the purified rRpMnSOD was 3299 U mg^{-1}.

3.3.4. Biological properties of rRpMnSOD

To further understand the properties of rRpMnSOD xanthine/XOD reactions were assayed under different conditions. Although rRpMnSOD retained more than 70% of relative activity at 15 °C - 35 °C, its optimum activity was recorded to be at 20 °C (Fig. 8A). Purified rRpMnSOD exhibited a lower activity (<30%) up to neutral pH, which raised drastically reaching maximum at pH 9.0 (Fig. 8B). Under basic conditions, rRpMnSOD demonstrated to be potentially active and showed more than 80% of relative activity.

4. Discussion

SODs as a family of enzymes that catalyze the dismutation of $O_2^{\bullet -}$ to H_2O_2 and O_2 play a critical role against harmful consequences of oxidative stress and to prevent free radical induced cellular damage in biological systems. Different types of SOD members have been identified from diverse organisms of both prokaryotes and eukaryotes [20]. However, molecular information about the bivalvian SODs is much limited compared to the mammalian SODs. In the present study, we identified two distinct members of SOD family, a MnSOD (RpMnSOD) and a Cu/ZnSOD (RpCu/ZnSOD) which was similar to a previously reported partially characterized isoform [14], from a commercially important aquatic species, Manila clam *R. philippinarum*. A comparative analysis was conducted in order to characterize these two enzymes at molecular level and to understand their *in vivo* functional coordination in performing mutual roles as antioxidant enzymes.

4.1. In silico analysis of RpSODs' molecular architecture and phylogeny

The cDNAs coding for *RpMnSOD* and *RpCu/ZnSOD* were translated to 226 and 154 amino acid long putative peptides,

Fig. 2. Alignment of *R. philippinarum* (A) MnSOD and (B) Cu/ZnSOD polypeptide sequences with corresponding known orthologs. The scale bar refers to the amino acid residues of RpMnSOD or RpCu/ZnSOD. Dots refer to the identity with RpMnSOD or Rp/CuZnSOD. Gaps introduced for optimal alignment are indicated with hyphens, and letters represent amino acids where substitutions occur. Conserved SOD-family signature motifs are gray shaded. GenBank accession number of each sequence is indicated. (A) MTS is boxed. Putative Mn^{2+}-binding sites are marked with asterisks (*). Secondary structure is assigned from the crystallographic structure of human mMnSOD (PDB ID, 1luvB) and is reported as α helixes (α), bridges (B) and β strands (β). (B) Putative Cu^{2+}- and Zn^{2+}-binding sites are marked with ● and ☼, respectively and two C residues forming a disulfide bridge are shown with arrows (↓). Secondary structure is assigned from the crystallographic structure of human Cu/ZnSOD (PDB ID, 1N19B) and is reported as α helixes (α) and β strands (β).

respectively. These RpSOD proteins revealed several common features of SOD family. The domain architecture of RpMnSOD was composed of a MTS, two Sod_Fe domains in N- and C-terminals, three MnSOD-family signature motifs and four Mn^{2+}-binding sites (Fig. 1A, C). Whereas, RpCu/ZnSOD possessed two Cu/ZnSOD-family signature motifs and minimum of seven residues responsible for Cu^{2+} and/or Zn^{2+}-binding activity (Fig. 1B, D). Two *N*-glycosylation sites were also predicted in both RpSODs, indicating that they might be glycoproteins as shown in other orthologs.

The MnSOD and Cu/ZnSOD are encoded by distinct genes. In general, MnSOD is synthesized as a precursor protein in the cytosol and its energy-dependent translocation into mitochondrial matrix is mediated by MTS. The premature MnSOD is proteolytically cleaved within mitochondria to form a mature protein. The mitochondrial matrix is the principal site generating the energy and $O_2^{\bullet-}$. MnSOD is the chief antioxidant enzyme in mitochondrial matrix of aerobic eukaryotes. Also, evidence of cytosolic MnSOD isoforms without MTS (cytosolic forms) have been identified in several species indicating their significance as antioxidant enzymes in the entire cellular compartment [12,21,22]. However, it was hypothesized that mitochondrial isoform could play more significant role than cytosolic form, since it may involve in protecting the mitochondrial DNA and membranes from ROS formed within mitochondria itself [9]. On the other hand, Cu/ZnSOD could be located in either cytosol or directed to the extracellular matrix. The RpMnSOD possessed a MTS of 26 residues at N-terminus indicating that it could be a mitochondrial matrix protein. No significant sequence conservation was found in MTS region of different lineages (Fig. 2A). It has been suggested that these divergent sequences of MTS in different species may retain the same functional attributes through specific motif(s) [23]. In contrast to RpMnSOD, RpCu/ZnSOD that lacks a signal peptide was suggested to be an intracellular protein.

The homology analysis revealed that two RpSODs demonstrated an average identity of ~65% (Table 2). Interestingly, RpMnSOD and RpCu/ZnSOD shared 65.2% and 63.9% of identity with the respective human SODs. The structural conservation of these two SOD members throughout the evolution was further supported by our alignment studies. The family signatures and the ion combining sites of RpSODs were completely conserved (Fig. 2).

Prokaryotic MnSODs typically form dimeric structures. Whereas, eukaryotes possess tetrameric MnSODs. A previous study compared different MnSODs by means of 3D structures and revealed a higher identity among them [24]. The 3D structural comparison of scallop MnSOD to that of human and *Aspergillus* demonstrated that molluscan MnSOD was more similar to human MnSOD [25]. We examined the secondary structural features of two RpSODs and subsequently constructed their 3D structures by homology modeling approach based on human SOD templates whose structure was elucidated via X-ray diffraction analysis [26]. The RpMnSOD was composed of 11 α helixes and 3 β strands (Fig. 2A). The invariant active site with the Mn^{2+} that is coordinated in a trigonal bipyramidal geometry to four liganding residues of MnSOD (H^{52}, H^{100}, D^{185} and H^{189}) and the water solvent ligand were found in its structural core (Fig. 3A–B). The water molecule bound with Mn^{2+} in active site cavity interacts with side chains of conserved residues such as Y^{60} and Q^{169}, and forms a hydrogen-bonded network that facilitates the proton transferring process when $O_2^{\bullet-}$ is reduced to H_2O_2 [27]. It was also intimated that the noticed α1 helical confirmation is required to juxtapose H^{52}, H^{56} and Y^{60} in an arrangement which is essential for catalytic mechanism [28]. The structure of RpCu/ZnSOD was made up of 2 α helixes and a β-barrel motif of 8 β strands (Fig. 2B) which was similar to its orthologs of Apo [29] and sea bass [30]. The dimeric Cu/ZnSOD contains two monomeric subunits with active sites harboring a Cu^{2+} and Zn^{2+} bridged by H^{63}. The Cu^{2+} is proposed to be the redox-metal for catalysis and Zn^{2+} appears to be important in maintaining overall enzyme stability [27]. While Cu^{2+} is coordinated by 3 H residues (H^{46}, H^{48} and H^{120}) and a water molecule in addition to H^{63}, Zn^{2+} is bound to H^{71}, H^{80} and D^{83} (Fig. 3C–E). These conserved residues are indispensable for both structure and function of Cu/ZnSOD and are also likely associated with stabilizing its confirmation under different conditions [31]. Collectively, these evidences suggest that the two SODs identified in this study from Manila clam could play the similar roles as in other biological systems, based on their conserved essential structural characteristics of known SOD orthologs.

The topology of the phylogenetic tree of MnSOD split into two branches based on subcellular localization, where RpMnSOD was placed within molluscan monophyletic clade (Fig. 4A). The evolutionary analysis of Cu/ZnSODs indicated a higher phylogenetic proximity between RpCu/ZnSOD and its surf clam homolog (Fig. 4B). The strength of phylogenetic relationship between their orthologs was found to be distinct in two trees. The MnSOD members exhibited a strong relationship among them. However, a weak relationship was an apparent feature among Cu/ZnSOD orthologs. This discrepancy could be based on their differences in characteristics, such as location and the active site topology [5], and leading to altered rates in evolution of these two SOD genes. Indeed, these SODs were believed to be independently evolved, of which Cu/ZnSOD exhibited an erratic rate of evolutionary divergence, compared to MnSOD that showed a relatively constant rate of evolution [32].

4.2. Comparative mRNA expressional profiling of RpSODs

We quantified the mRNA content of the *SOD*s in different tissues of healthy clams by qRT-PCR. Although, the transcripts of two *SOD*s were ubiquitously detected in all examined tissues at different levels, they were significantly higher in gills and hemocytes (Fig. 5). The distribution profile of *RpMnSOD* was similar to that reported for the *MnSOD* in blood clam [33]. Moreover, *ECSOD*s in bay scallop [13] and mud crab [34] have also demonstrated highest expression level in hemocytes as observed for *RpMnSOD*. The spatial expression pattern of *RpCu/ZnSOD* was analogous to those of bay scallop [35] and Zhikong scallop [31] that revealed highest expression in gills. However, the *RpSOD* expression profiles were somewhat different from few previous reports in other animals, such as Hong Kong oyster [10] and a hydrothermal crab [36] that express an abundant amount of *SOD*s in muscle. All these data collectively suggest that transcriptional profiles of *SOD*s are subtype- and species-dependent. In particular, differential expression of *MnSOD* was tissue-specific and proposed to be associated with relative content of mitochondria and oxidative load, as it is the principal antioxidant scavenger of ROS generated during aerobic respiration [37].

In filter feeders like bivalves, the gills are most susceptible for infections as they play a role in flushing water that possibly contains pathogens, waterborne toxins and pollutants (which could cause oxidative stress). The remarked constitutive expression of *SOD*s in gills implied their substantial physiological role(s) against the pathogen invasion and protecting the host from oxidative damage. Meanwhile, hemocytes are widely recognized vital role players in innate immune system of molluscs [38], and substantial *SOD* expression in hemocytes suggested that *RpSOD*s might be involved in defense response of clam against stressors.

The *SOD*s are considered to be common stress-responsive elements of defense system whose mRNA expression could be modulated by various factors including environmental changes, chemical pollutants (heavy metals) and biological stimuli (pathogens) [5]. In this study, we compared the *RpSOD* mRNA expression as a protective mechanism against oxidative stress caused by mitogen- and pathogen-injection by qRT-PCR and report the time-dependent expression profiles of *RpSOD*s in clam challenged by poly I:C,

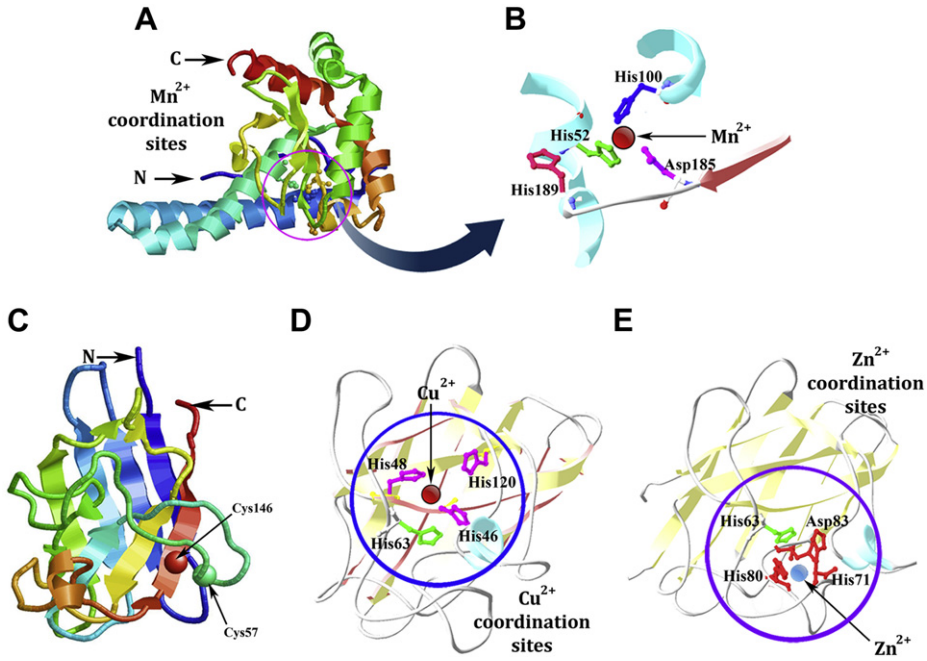

Fig. 3. The predicted 3D structures of *R. philippinarum* MnSOD (A–B) and Cu/ZnSOD (C–E). (A) Ribbon diagram of RpMnSOD and location of Mn^{2+} liganding active site and (B) magnified view of Mn^{2+}-interactive amino acid residues. (C) Ribbon diagram of RpCu/ZnSOD. Disulfide bridge forming Cys residues are marked. (D) Cu^{2+}-interactive His residues and (E) Zn^{2+}-interactive amino acid residues in RpCu/ZnSOD are shown. N, amino terminal; C, carboxy terminal.

a common viral mimic, LPS endotoxin, a component of Gram negative bacteria and a *V. tapetis*, a Gram negative species, belonging to *Vibrio* genus causing massive mortalities in global bivalve production [1]. Our results indicated that these experimental injections significantly altered the transcription of both *RpSOD*s in gills and hemocytes of challenged clams. In fact, the *SOD* expression patterns varied in terms of magnitude and kinetics with different challenging agents and the tissue type.

The poly I:C induced the transcription of *RpSOD*s to maxima at mid- and late-phases in gill and hemocytes, respectively (Fig. 6A, B).

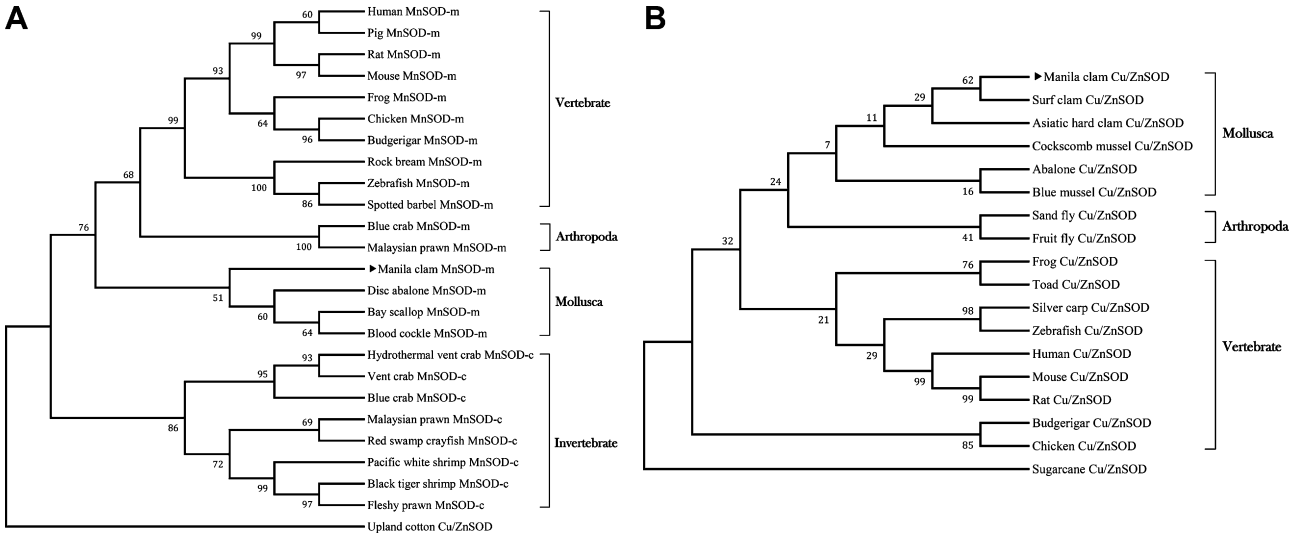

Fig. 4. Phylogenetic relationship of *R. philippinarum* (A) MnSOD and (B) Cu/ZnSOD with other MnSOD and Cu/ZnSOD members, respectively on the basis of amino acid sequences using Neighbor-Joining distance analysis. The topological stability of the trees was evaluated by 5000 bootstrap replications and bootstrap percentages are shown on interior branches. (A) The tree was rooted with a Cu/ZnSOD from upland cotton (ACC93639). The GenBank accession numbers of sequences used here are as follows: Human MnSOD-m (NP_000627); Pig MnSOD-m (NP_999292); Rat MnSOD-m (NP_058747); Mouse MnSOD-m (AAB60902); Frog MnSOD-m (AAQ63483); Chicken MnSOD-m (NP_989542); Budgerigar MnSOD-m (AAO72712); Rock bream MnSOD-m (JN593103); Zebra fish MnSOD-m (NP_956270); Spotted barbel MnSOD-m (ACR23311); Blue crab MnSOD-m (AAF74770); Malaysian prawn MnSOD-m (AAZ81617); Manila clam MnSOD-m (JN593115); Disc abalone MnSOD-m (ABF67504); Bay scallop MnSOD-m (ABW98672); Blood cockle MnSOD-m (ADC34695); Hydrothermal vent crab MnSOD-c (CAR85668); Vent crab MnSOD-c (CAR85669); Blue crab MnSOD-c (AAF74771); Malaysian prawn MnSOD-c (AAY79405); Red swamp crayfish MnSOD-c (ABX44762); Pacific white shrimp MnSOD-c (AAY57407); Black tiger shrimp MnSOD-c (AAW50395); Fleshy prawn MnSOD-c (ACS49842). "c" and "m" stand for cytosolic and for mitochondrial, respectively. (B) The tree was rooted with sugarcane Cu/ZnSOD (ACT53877). The GenBank accession numbers of sequences used here are as follows: Manila clam Cu/ZnSOD (JQ362416); Surf clam Cu/ZnSOD (ACU46013); Cockscomb mussel Cu/ZnSOD (ACI28282); Asiatic hard clam Cu/ZnSOD (ACZ95447); Abalone Cu/ZnSOD (ABF67508); Blue mussel Cu/ZnSOD (CAE46443); Sand fly Cu/ZnSOD (ADH94607); Fruit fly Cu/ZnSOD (Q9U4X4); Frog Cu/ZnSOD (NP_001080933); Toad Cu/ZnSOD (ABD75370); Silver carp Cu/ZnSOD (ADJ67808); Zebra fish Cu/ZnSOD (NP_571369); Human Cu/ZnSOD (NP_000445); Mouse Cu/ZnSOD (NP_035564); Rat Cu/ZnSOD (NP_058746); Budgerigar Cu/ZnSOD (AAO72711); Chicken Cu/ZnSOD (AAB88059).

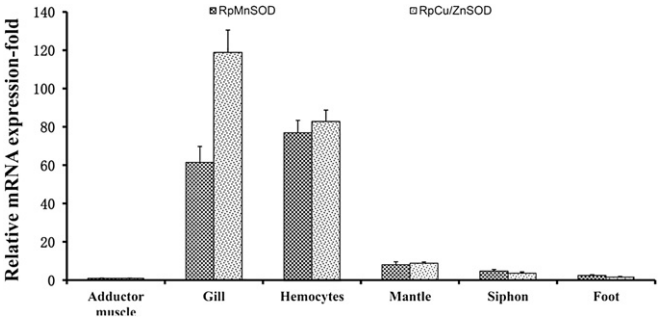

Fig. 5. Spatial expressional analysis of differentially distributed *R. philippinarum SOD* transcripts using SYBR green qRT-PCR. The relative *RpSOD* mRNA expression in each tissue was calculated by the $2^{-\Delta\Delta CT}$ method using Manila clam *β-actin* as reference gene and adductor muscle as a calibrator. Vertical bars represent the S.D. ($n = 5$).

Previous reports demonstrated the changes of *SOD* expression in shrimp, when live WSSV was injected. In white shrimp, *ECSOD* [8] and *cMnSOD* [12] were shown to be upregulated at early phase. In contrast, *mMnSOD* of Chinese shrimp exhibited a downregulation at late phase [9]. The oxidative stress caused during viral infection in mammals is well established [39]. The transient systemic response elicited by *RpSOD*s against poly I:C is an evidence for their involvement in antiviral defense in clam.

A distinct peaked expression of *RpSOD*s was detected at 3 h and 6 h p.i. of LPS in gills and hemocytes, respectively (Fig. 6C, D). The dose-dependency of LPS-induced expression has been reported for *MnSOD* of *Hemibarbus mylodon* [6] and *ecCu/ZnSOD* of blue crab [7]. In addition, the temporal expression of *RpSOD*s upon LPS p.i. was congruent with earlier findings in bay scallop [40] and bumblebee [41]. The LPS-mediated endotoxic shock and subsequent oxidative

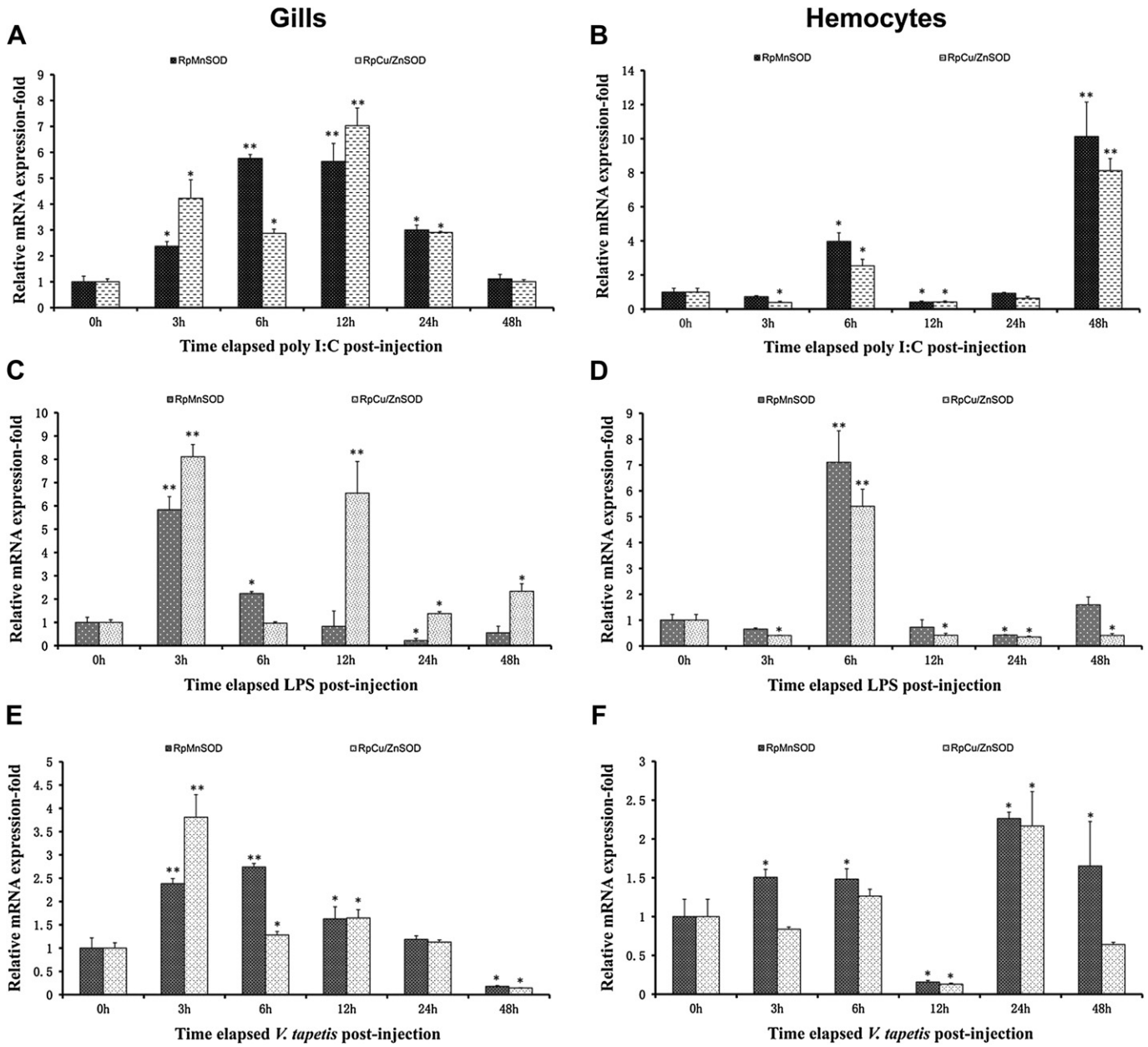

Fig. 6. Temporal expressional analysis of *R. philippinarum SOD* transcripts in gills (A, C, E) and hemocytes (B, D, F) of poly I:C (A, B), LPS (C, D) and *V. tapetis* (E, F) -injected animals, respectively, using SYBR green qRT-PCR. The relative *RpSOD* mRNA expression in each tissue was calculated by the $2^{-\Delta\Delta CT}$ method using Manila clam *β-actin* as reference gene. Then, *RpSOD* expression was normalized to its expression in the respective time-matched saline-injected control (expression >1 means up-regulated; whereas <1 means down-regulated). Vertical bars represent the S.D. ($n = 5$). The asterisk symbols, * and ** represent statistical difference in expression when compared with uninjected (0 h) animal at normal ($P < 0.05$) and extreme ($P < 0.01$) levels, respectively.

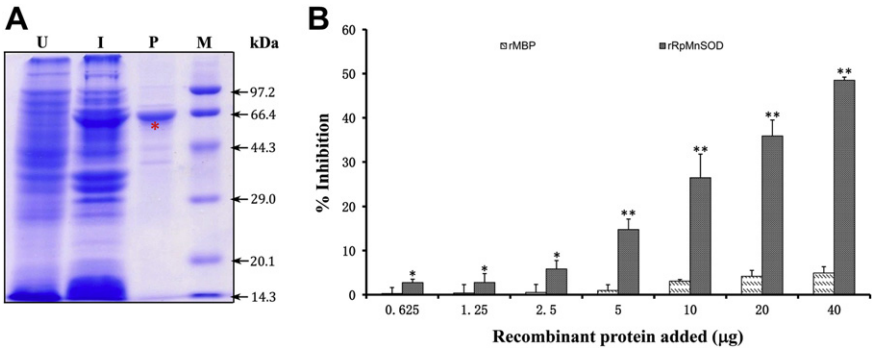

Fig. 7. (A) Expression of *R. philippinarum* MnSOD/MBP protein in *E. coli* BL21 (DE3) induced by IPTG and purification using amylose resin affinity chromatography. Lanes: U, total cellular extracts from *E. coli* BL21 (DE3) containing recombinant plasmid before IPTG induction; I, after IPTG induction (0.25 mM) at 17 °C for 20 h; P, the purified recombinant fusion protein (marked with *); M, low molecular weight protein marker (Takara). (B) Determination of SOD activity and antioxidant potential of *Ruditapes philippinarum* rRpMnSOD using xanthine/XOD method. Enzymatic activity was quantified as described in Section 2.9 in the presence of increasing amounts of rRpMnSOD. The columns represent the percent inhibition of rMBP, rRpMnSOD, respectively. Vertical bars represent the S.D. ($n = 3$). The asterisk symbols, * and ** represent statistical difference when compared with MBP at normal ($P < 0.05$) and extreme ($P < 0.01$) levels, respectively.

damage is understood in mammals [42]. Moreover, the ascended *SOD* mRNA level is proposed to be a part of antioxidant defense mechanism to scavenge and mitigate the augmented levels of LPS-induced $O_2^{\bullet-}$ [43]. In fact, an earlier finding indicated that LPS-induced TNF-α secretion and *SOD* expression occurred via ERK1 activation and, defined the intra-network between *SOD*, TNF-α and their subsequent activities during inflammation [44]. We have identified the Manila clam *TNF-α* from our cDNA library (GenBank Accession. JX025641). Transcriptional analysis of *TNF-α* after the immune challenges (Section 2.4) demonstrated a coincided pattern of *RpSODs* and *RpTNF-α* mRNA expression in hemocytes (Y. Lee et. al, manuscript under preparation). TNF-α was found to induce the MnSOD expression pre-translationally and confers protection against ROS [45,46]. Therefore, it is suggestive that *RpMnSOD* could be a cytokine-regulated gene. In light of these data, we speculate that pronounced expression of *RpSODs* is likely associated with their role in host protection against oxidative imbalance caused by LPS.

Not surprisingly, the *RpSOD* expression in the gills and hemocytes was also significantly affected by investigational challenge with *V. tapetis* (Fig. 6E, F). From 3 h to 12 h p.i. of *V. tapetis*, the gills manifested an increased RpSOD level with a subsequent depression in 48 h p.i. which was similar to a response demonstrated by two MnSODs in kuruma shrimp [22] and two SODs in Hong Kong oyster [10], against *Vibrio alginolyticus* injection. Moreover, different invading pathogens induced varying degree of toxicities, and generated different amounts of oxygen-derived products [12]. The dynamic expression kinetics of *RpSODs* was tissue specific and it might be attributed to the *in vitro* imbalance between the levels of ROS and *RpSOD* transcripts. While intensified *RpSOD* mRNA levels could lead to a successful elimination of ROS, steady reduction in *RpSOD* transcripts allows an elevation in ROS level to kill bacteria or to initiate signaling pathways via activating transcription factors such as NF-kB and AP1 [3].

When pathogen invasion occurs, molluscs elicit a series of immune defense responses. Phagocytosis is a major protective mechanism of hemocytes [2] which leads to an increased O_2 consumption and active production of ROS. In addition, host also manifests other immune responses through effector molecules such as lectins, antimicrobial peptides and lysozymes. In turn, all these processes will require more ATP to support the high energy demand leading to an elevated ROS production and finally resulting mitochondrial oxidative load. Our data together with diverse expressional studies carried out in crustacean [8], molluscan [13,14,24,31,35] and fish [6,30] species strongly suggest possible pivotal role(s) for SODs in quenching the bacterial-induced ROS and successive oxidative stress. In addition, cytosolic Cu/ZnSOD has been implicated with a protective mechanism under pathological condition by preventing the formation of a toxic product known as peroxynitrite [35] which is formed from a coupling reaction between nitric oxide and $O_2^{\bullet-}$. In accordance with this hypothesis, increased RpCu/ZnSOD after immune challenges may be associated with extenuating the peroxynitrite- and ROS-toxicity.

This study further aids our understanding about intricate relationships among pathogen infections, oxidative imbalance, and host defense via antioxidant responses in clams. Although the underlying mechanisms behind the transcriptional profiles were not completely understood, based on the coordinated expression patterns of RpMnSOD and RpCu/ZnSOD after mitogen and bacterial

Table 3
Tryptic peptides sequenced by Nano-LC/ESI-MS/MS mass spectrometry.

Residues	Experimental Mr	Calculated Mr	Tryptic peptide sequence
1–16	2079.0282	2079.1108	RISEFMLSAQSVKLACVLPKV
17–24	–	–	SSLGAAGA (Missing)
25–56	3574.8524	3572.8337	RLKHTLPELPYEYSALEPVISNEIMQIHHQKH
55–71	1796.8542	1796.8441	KHHQTYVNNLNATEEKL
70–92	2269.2032	2268.2147	KLAEAMKNNDVAQVISLQPALKF
91–111	2139.0855	2137.0858	KFNGGGHINHSIFWQVLSPKG
112–123	–	–	GGSPSGDLLELI (Missing)
124–133	986.4489	986.4458	KRDYGSFDKM
132–161	3070.4558	3068.4597	KMKDMLTQASVGVQGSGWGWLGFNQLNGRL
162–197	4013.0253	4010.9917	RILTCANQDPLQPTTGFIPLFGIDVWEHAYYLQYKN
196–205	989.5305	989.5294	KNVRPDYVKA
204–219	1618.7728	1618.7740	KAIFDVANWEEVGNRL
218–224	557.3275	557.3285	RLAQARL
225–226	–	–	DA (Missing)

Mr; relative molecular weight, underlined; fragment of MBP fusion protein, shading; repetitive residues of preceding fragment.

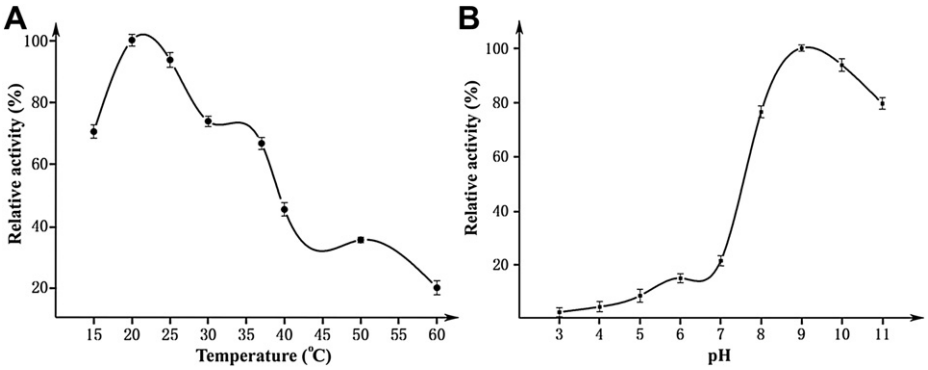

Fig. 8. Determination of optimum assay parameters for the SOD activity of *R. philippinarum* rRpMnSOD using xanthine/XOD method. Enzyme activity was quantified at different (A) temperatures (15–60 °C) and (B) pHs (3–11). Vertical bars represent the S.D. ($n = 3$).

injection, we infer that these two RpSODs may govern similar immune responses. However, future efforts are necessary to be conducted with other factors including environmental cues and potential microbes to gain an overall understanding of SODs' contribution in Manila clam physiology.

4.3. Functional characterization of recombinant RpMnSOD

Despite the progresses achieved in the transcriptional studies of *SOD*s, characterization of SOD proteins at functional level has not been well documented. We translated the RpMnSOD *in vitro* using *E. coli* BL21 system. In order to verify the deduced amino acid sequence, we experimentally determined the sequence of purified rRpMnSOD fusion protein using Nano-LC/ESI-MS/MS and confirmed its identity. To elucidate the antioxidant property, we engaged the rRpMnSOD in an antioxidant assay. The rRpMnSOD exhibited dose-dependency (Fig. 7B) with a specific activity of 3299 U mg^{-1} which was significantly higher than previously reported specific activities for molluscan MnSODs from abalone [47] and Antarctic bivalve [48] and a crustacean mMnSOD from Chinese shrimp [9]. However, it could be inferred that the native RpMnSOD should possess a higher activity than the recombinant RpMnSOD, as the recombinant protein cannot be expected to completely recover to its native folding.

The activity was also determined under different temperatures and pHs (Fig. 8A, B). A relative activity of >45% was retained by the rRpMnSOD even at 40 °C. The substantial survival of its activity in the temperature range from 15 to 40 °C indicated that RpMnSOD might be active against ROS generated due to thermal stress. The rRpMnSOD was more potent under alkaline condition compared to acidic condition, as reported for SODs of Antarctic bivalve [48] and bay scallop [35]. The metal–ligand interaction is highly sensitive to the pH of the medium. The imidazole rings of Mn^{2+} liganding His residues may become protonated at lower pHs. Thus, metal ligands could be considered as relatively stable in alkaline conditions when compared with acidic pHs [49] in which they might be lost due to weak-coordination. The high SOD activity demonstrated in our *in vitro* assay using xanthine/XOD system affirmed the potential role of RpMnSOD in effectively removing the dangerous levels of $O_2^{\bullet-}$.

Functional role of Manila clam antioxidant enzyme network including thioredoxins [50,51] and GSTs [15,52] studied earlier in our laboratory, and this study of SODs will aid in delineating the significance of these enzymes in establishing a balance in redox environment by scavenging ROS in clam physiology.

5. Conclusion

In conclusion, a *MnSOD* from Manila clam *R. philippinarum* was cloned and recombinantly expressed. The molecular architecture of RpMnSOD and RpCu/ZnSOD established through *in silico* characterization portrayed all essential features of SOD family of proteins. A comparative transcriptional profiling of *RpSOD*s manifested their higher expression in gills and hemocytes suggesting immunological importance in a tissue-specific manner. Investigational challenges revealed their synchronized dynamic expression in a tissue- and stimulant-dependent manner. Furthermore, demonstration of rRpMnSOD's antioxidant property affirmed the molecular characterization at the protein level. Finally, the transient mRNA-expressional responses of *RpSOD*s together with the activity of translated rRpMnSOD protein suggested that these SODs perhaps perform crucial role(s) in redox homeostasis and are involved in Manila clam host defense.

Acknowledgments

This work was supported by the Marine and Extreme Genome Research Center Program of the Ministry of Land, Transportation and Maritime Affairs, Republic of Korea.

Appendix A

Suppl. Table 1
Characteristic features of RpCu/ZnSOD.

Characteristic feature	Description for RpCu/ZnSOD
Length of complete cDNA	1567 bp
5′-UTR	108 bp
3′-UTR	994 bp
CDS	465 bp
Putative polyadenylation signal	^{649}AATATA^{654}
Length of polypeptide	154 amino acids
Molecular mass	15817.6 Da
*p*I	6.02
Signal peptide	Absent
Localization	Cytoplasm
Disulfide bond	C^{57}-C^{146}
N-glycosylation sites	^{86}NVTA^{89} and ^{98}NITD^{101}
Cu/ZnSOD-family Signature motifs	^{44}GFHVHAFGDNS^{54} ^{138}GNAGGRLACGVI^{149}
Putative metal-binding sites	Cu^{2+}: H^{46}, H^{48}, H^{63}, and H^{120} Zn^{2+}: H^{63}, H^{71}, H^{80} and D^{83}

References

[1] Park K-I, Paillard C, Le Chevalier P, Choi K-S. Report on the occurrence of brown ring disease (BRD) in Manila clam, *Ruditapes philippinarum*, on the west coast of Korea. Aquaculture 2006;255:610–3.
[2] Reade PC. Phagocytosis in invertebrates[ast]. Aust J Exp Biol Med 1968;46:219–29.
[3] Schreck R, Rieber P, Baeuerle PA. Reactive oxygen intermediates as apparently widely used messengers in the activation of the NF-kappa B transcription factor and HIV-1. The EMBO Journal 1991;10:2247–58.

[4] Fridovich I. Superoxide radical and superoxide dismutases. Annu Rev Biochem 1995;64:97–112.
[5] Zelko IN, Mariani TJ, Folz RJ. Superoxide dismutase multigene family: a comparison of the CuZn-SOD (SOD1), Mn-SOD (SOD2), and EC-SOD (SOD3) gene structures, evolution, and expression. Free Radical Biology & Medicine 2002;33:337–49.
[6] Cho YS, Lee SY, Bang IC, Kim DS, Nam YK. Genomic organization and mRNA expression of manganese superoxide dismutase (Mn-SOD) from *Hemibarbus mylodon* (Teleostei, Cypriniformes). Fish Shellfish Immunol 2009;27:571–6.
[7] Sook Chung J, Bachvaroff TR, Trant J, Place A. A second copper zinc superoxide dismutase (CuZnSOD) in the blue crab *Callinectes sapidus*: cloning and up-regulated expression in the hemocytes after immune challenge. Fish Shellfish Immunol 2012;32:16–25.
[8] Tian J, Chen J, Jiang D, Liao S, Wang A. Transcriptional regulation of extracellular copper zinc superoxide dismutase from white shrimp *Litopenaeus vannamei* following *Vibrio alginolyticus* and WSSV infection. Fish Shellfish Immunol 2011;30:234–40.
[9] Zhang Q, Li F, Wang B, Zhang J, Liu Y, Zhou Q, et al. The mitochondrial manganese superoxide dismutase gene in Chinese shrimp Fenneropenaeus chinensis: cloning, distribution and expression. Developmental & Comparative Immunology 2007;31:429–40.
[10] Yu Z, He X, Fu D, Zhang Y. Two superoxide dismutase (SOD) with different subcellular localizations involved in innate immunity in *Crassostrea hongkongensis*. Fish Shellfish Immunol 2011;31:533–9.
[11] Bao Y, Li L, Zhang G. The manganese superoxide dismutase gene in bay scallop *Argopecten irradians*: cloning, 3D modelling and mRNA expression. Fish & Shellfish Immunology 2008;25:425–32.
[12] Gomez-Anduro GA, Barillas-Mury CV, Peregrino-Uriarte AB, Gupta L, Gollas-Galvan T, Hernandez-Lopez J, et al. The cytosolic manganese superoxide dismutase from the shrimp *Litopenaeus vannamei*: molecular cloning and expression. Dev Comp Immunol 2006;30:893–900.
[13] Bao Y, Li L, Wu Q, Zhang G. Cloning, characterization, and expression analysis of extracellular copper/zinc superoxide dismutase gene from bay scallop *Argopecten irradians*. Fish Shellfish Immunol 2009;27:17–25.
[14] Li C, Sun H, Chen A, Ning X, Wu H, Qin S, et al. Identification and characterization of an intracellular Cu, Zn-superoxide dismutase (icCu/Zn-SOD) gene from clam *Venerupis philippinarum*. Fish Shellfish Immunol 2010;28:499–503.
[15] Umasuthan N, Revathy KS, Lee Y, Whang I, Choi CY, Lee J. A novel molluscan sigma-like Glutathione S-Transferase from Manila clam, *Ruditapes philippinarum*: cloning, characterization and transcriptional profiling. Comparative Biochemistry and Physiology Part C: Toxicology & Pharmacology.
[16] Arnold K, Bordoli L, Kopp J, Schwede T. The SWISS-MODEL workspace: a web-based environment for protein structure homology modelling. Bioinformatics 2006;22:195–201.
[17] Roy A, Kucukural A, Zhang Y. I-TASSER: a unified platform for automated protein structure and function prediction. Nature Protocols 2010;5:725–38.
[18] Maina CV, Riggs PD, Grandea 3rd AG, Slatko BE, Moran LS, Tagliamonte JA, et al. An *Escherichia coli* vector to express and purify foreign proteins by fusion to and separation from maltose-binding protein. Gene 1988;74:365–73.
[19] Nagai T, Inoue R, Inoue H, Suzuki N. Preparation and antioxidant properties of water extract of propolis. Food Chemistry 2003;80:29–33.
[20] Bannister JV, Bannister WH, Rotilio G. Aspects of the structure, function, and applications of superoxide dismutase. CRC Critical Reviews in Biochemistry 1987;22:111–80.
[21] Gomez-Anduro GA, Sotelo-Mundo RR, Muhlia-Almazan A, Yepiz-Plascencia G. Tissue-specific expression and molecular modeling of cytosolic manganese superoxide dismutases from the white shrimp Litopenaeus vannamei. Dev Comp Immunol 2007;31:783–9.
[22] Lin YC, Lee FF, Wu CL, Chen JC. Molecular cloning and characterization of a cytosolic manganese superoxide dismutase (cytMnSOD) and mitochondrial manganese superoxide dismutase (mtMnSOD) from the kuruma shrimp *Marsupenaeus japonicus*. Fish Shellfish Immunol 2010;28:143–50.
[23] Kong BW, Kim H, Foster DN. Expression analysis and mitochondrial targeting properties of the chicken manganese-containing superoxide dismutase. Biochim Biophys Acta 2003;1625:98–108.
[24] Bao Y, Li L, Zhang G. The manganese superoxide dismutase gene in bay scallop *Argopecten irradians*: cloning, 3D modelling and mRNA expression. Fish Shellfish Immunol 2008;25:425–32.
[25] Ikebuchi M, Takeuchi K, Yamane T, Ogikubo O, Maeda T, Kimura H, et al. Primary structure and properties of Mn-superoxide dismutase from scallop adductor muscle. Int J Biochem Cell Biol 2006;38:521–32.
[26] Borgstahl GE, Parge HE, Hickey MJ, Beyer Jr WF, Hallewell RA, Tainer JA. The structure of human mitochondrial manganese superoxide dismutase reveals a novel tetrameric interface of two 4-helix bundles. Cell 1992;71:107–18.
[27] Abreu IA, Cabelli DE. Superoxide dismutases-a review of the metal-associated mechanistic variations. Biochim Biophys Acta 2010;1804:263–74.
[28] Stallings WC, Pattridge KA, Strong RK, Ludwig ML. The structure of manganese superoxide dismutase from *Thermus thermophilus* HB8 at 2.4-A resolution. J Biol Chem 1985;260:16424–32.
[29] Banci L, Bertini I, Cramaro F, Del Conte R, Viezzoli MS. Solution structure of Apo Cu, Zn superoxide dismutase: role of metal ions in protein folding. Biochemistry 2003;42:9543–53.
[30] Chakravarthy N, Aravindan K, Kalaimani N, Alavandi SV, Poornima M, Santiago TC. Intracellular Copper Zinc Superoxide dismutase (icCuZnSOD) from Asian seabass (Lates calcarifer): molecular cloning, characterization and gene expression with reference to *Vibrio anguillarum* infection. Dev Comp Immunol 2012;36:751–5.
[31] Ni D, Song L, Gao Q, Wu L, Yu Y, Zhao J, et al. The cDNA cloning and mRNA expression of cytoplasmic Cu, Zn superoxide dismutase (SOD) gene in scallop Chlamys farreri. Fish Shellfish Immunol 2007;23:1032–42.
[32] Smith MW, Doolittle RF. A comparison of evolutionary rates of the two major kinds of superoxide dismutase. Journal of Molecular Evolution 1992;34:175–84.
[33] Li C, He J, Su X, Li T. A manganese superoxide dismutase in blood clam Tegillarca granosa: molecular cloning, tissue distribution and expression analysis. Comparative Biochemistry and Physiology Part B, Biochemistry & Molecular Biology 2011;159:64–70.
[34] Lin Y-C, Vaseeharan B, Chen J- C. Identification of the extracellular copper–zinc superoxide dismutase (ecCuZnSOD) gene of the mud crab Scylla serrata and its expression following β-glucan and peptidoglycan injections. Molecular Immunology 2008;45:1346–55.
[35] Bao Y, Li L, Xu F, Zhang G. Intracellular copper/zinc superoxide dismutase from bay scallop *Argopecten irradians*: Its gene structure, mRNA expression and recombinant protein. Fish & Shellfish Immunology 2009;27:210–20.
[36] Marchand J, Leignel V, Moreau B, Chenais B. Characterization and sequence analysis of manganese superoxide dismutases from Brachyura (*Crustacea: Decapoda*): hydrothermal Bythograeidae versus littoral crabs. Comparative Biochemistry and Physiology Part B, Biochemistry & Molecular Biology 2009;153:191–9.
[37] Benard G, Faustin B, Passerieux E, Galinier A, Rocher C, Bellance N, et al. Physiological diversity of mitochondrial oxidative phosphorylation. American Journal of Physiology Cell Physiology 2006;291:C1172–82.
[38] Donaghy L, Lambert C, Choi K-S, Soudant P. Hemocytes of the carpet shell clam (*Ruditapes decussatus*) and the Manila clam (*Ruditapes philippinarum*): current knowledge and future prospects. Aquaculture 2009;297:10–24.
[39] Kathleen BS. Oxidative stress during viral infection: a review. Free Radical Biology and Medicine 1996;21:641–9.
[40] Bao Y, Li L, Xu F, Zhang G. Intracellular copper/zinc superoxide dismutase from bay scallop *Argopecten irradians*: its gene structure, mRNA expression and recombinant protein. Fish Shellfish Immunol 2009;27:210–20.
[41] Choi YS, Lee KS, Yoon HJ, Kim I, Sohn HD, Jin BR. Bombus ignitus Cu, Zn superoxide dismutase (SOD1): cDNA cloning, gene structure, and up-regulation in response to paraquat, temperature stress, or lipopolysaccharide stimulation. Comparative Biochemistry and Physiology Part B, Biochemistry & Molecular Biology 2006;144:365–71.
[42] Abe R, Shimosegawa T, Moriizumi S, Kikuchi Y, Kimura K, Satoh A, et al. Lipopolysaccharide induces manganese superoxide dismutase in the Rat Pancreas: its role in Cerulein Pancreatitis. Biochemical and Biophysical Research Communications 1995;217:1216–22.
[43] Lee S-J, Lim K- T. UDN glycoprotein regulates activities of manganese-superoxide dismutase, activator protein-1, and nuclear factor-κB stimulated by reactive oxygen radicals in lipopolysaccharide-stimulated HCT-116 cells. Cancer Letters 2007;254:274–87.
[44] Marikovsky M, Ziv V, Nevo N, Harris-Cerruti C, Mahler O. Cu/Zn superoxide dismutase plays important role in immune response. J Immunol 2003;170: 2993–3001.
[45] Wong GH, Goeddel DV. Induction of manganous superoxide dismutase by tumor necrosis factor: possible protective mechanism. Science 1988;242:941–4.
[46] Warner BB, Burhans MS, Clark JC, Wispe JR. Tumor necrosis factor-alpha increases Mn-SOD expression: protection against oxidant injury. Am J Physiol 1991;260:L296–301.
[47] Ekanayake PM, Kang H-S, De Zyosa M, Jee Y, Lee Y-H, Lee J. Molecular cloning and characterization of Mn-superoxide dismutase from disk abalone (*Haliotis discus discus*). Comparative Biochemistry and Physiology Part B: Biochemistry and Molecular Biology 2006;145:318–24.
[48] Park H, Ahn I-Y, Lee JK, Shin SC, Lee J, Choy E- J. Molecular cloning, characterization, and the response of manganese superoxide dismutase from the Antarctic bivalve *Laternula elliptica* to PCB exposure. Fish & Shellfish Immunology 2009;27:522–8.
[49] Dolashki A, Abrashev R, Stevanovic S, Stefanova L, Ali SA, Velkova L, et al. Biochemical properties of Cu/Zn-superoxide dismutase from fungal strain *Aspergillus niger* 26. Spectrochimica Acta Part A: Molecular and Biomolecular Spectroscopy 2008;71:975–83.
[50] Umasuthan N, Saranya Revathy K, Lee Y, Whang I, Lee J. Mitochondrial thioredoxin-2 from Manila clam (*Ruditapes philippinarum*) is a potent anti-oxidant enzyme involved in antibacterial response. Fish & Shellfish Immunology 2012;32:513–23.
[51] Revathy KS, Umasuthan N, Lee Y, Whang I, Kim HC, Lee J. Cytosolic thioredoxin from *Ruditapes philippinarum*: molecular cloning, characterization, expression and DNA protection activity of the recombinant protein. Dev Comp Immunol 2012;36:85–92.
[52] Saranya Revathy K, Umasuthan N, Lee Y, Choi CY, Whang I, Lee J. First molluscan theta-class Glutathione S-Transferase: identification, cloning, characterization and transcriptional analysis post immune challenges. Comparative Biochemistry and Physiology Part B: Biochemistry and Molecular Biology 2012;162:10–23.